ICSV13 - Vienna
The Thirteenth International Congress on Sound and Vibration
Vienna, Austria, July 2-6, 2006

STABILITY ANALYSIS OF A THREE-BALL AUTOMATIC BALANCER

Chung-Jen Lu* and Chia-Hsing Hung

Department of Mechanical Engineering
National Taiwan University
No. 1 Roosevelt Rd. Sec. 4
Taipei 10617, Taiwan
E-mail: cjlu@ntu.edu.tw

Abstract

Ball-type automatic balancers can effectively reduce the vibrations of an optical disk drive due to the inherent imbalance of the optical disk. Although ball-type automatic balancers used in practice consists of several balls moving freely along a circular orbit, no studies have investigated the dynamic characteristics of ball-type balancers with more than two balls. This paper aims to study the dynamic stability of a three-ball automatic balancer. Emphasis is put on the stability of the equilibrium positions of the balls where the disk is perfectly balanced. A theoretical model of an optical disk drive packed with a three-ball automatic balancer is constructed first. The governing equations of the theoretical model are derived using Lagrange's equations. Closed-form formulae for the equilibrium positions are presented. Stability of the perfect balancing equilibrium positions is investigated by the center manifold theorem. The theoretic results are verified by numerical analysis.

INTRODUCTION

Optical disk drives have been widely used for data storage. The speed of the spindle has been brought up to 10,000 rmp to increase the data transfer rate. At such a high rotating speed, the optical disk drive may suffer from serious vibrations due to the eccentricity of the optical disk used. Since the unbalance varies from disk to disk, it is desirable to have an automatic balancer system (ABS) equipped with the optical disk drive that can eliminate the unbalance associated with each disk automatically. The most popular ABS adopted by optical disk drive industry is the ball-type ABS. A ball-type ABS consists of several balls moving freely in a circular groove. Under proper working conditions, the balls will settle at the positions such that the vibration due to the eccentric mass of the disk can be totally suppressed. These particular positions are

called the perfect balancing positions henceforth. The performance of the ABS is closely related to the stable regions of the perfect balancing positions.

Although the ball-type balancers currently used in practice consists of several balls, much work has been done on the dynamics characteristics of a single-ball or two-ball balancers. Bövik and Högford [1] analyzed the stability of the perfect balancing position by the method of multiple scales. Rajalingham et al. [2] investigated the nonlinear system consists of an undamped rotor and a single-ball ABS. The stability of the equilibrium position was determined by the corresponding linearized system. Lee and Moorhem [3] numerically determined the stable region for perfect balancing by the Floquet theory. Chung and Ro [4] and Kang et al. [5] investigated the stability of a two-ball ABS comprehensively. The stability was checked with the variations for a pair of design parameters. Huang et al. [6] studied the dynamic characteristics of a single-ball ABS. Kim et al. [7] investigated the dynamic behaviour of a two-ball balancer based on a three-dimensional model. Chao et al. [8] evaluated the performance of a two-ball balancer with consideration of the in-plane rotational motions. To the best of the authors' knowledge, no researchers have investigated the effects of the number of balls on the performance of ball-type automatic balancers.

In the present paper, we study the stability of the perfect balancing positions of a rotating disk equipped with a three-ball ABS. The nonlinear equations of motion are derived with respect to a rotating coordinate system. Equilibrium positions and the associated linearized equations are derived. Stable areas of the perfect balancing positions on a parametric plane are identified using the center manifold theorem. Finally, time responses of the system are computed to verify the analytic results.

MATHEMATICAL MODEL AND GOVERNING EQUATIONS

Figure 1 shows the schematic of the ABS-rotor system and the rotating reference frame. The ABS is composed of a circular disk with a groove containing balls and a damping fluid. The balls move freely along the groove, subjected to viscous damping only. The radius of the groove is δ. The rotor consists of an unbalanced rotating disk and the suspension system. The disk with mass m_d rotates with a constant angular velocity ω. The mass center *G* of the disk is located a distance *e* from the disk's geometric center *C*. The flexibility of the suspension system is characterized by equivalent linear springs and viscous dampers, denoted by $\left(k_x, k_y\right)$ and $\left(c_x, c_y\right)$, respectively. For simplicity, we assume that $k_x = k_y = K$, $c_x = c_y = C$.

The *xy*-reference frame rotates with the rotor speed ω. The center *C* of the disk is located at the origin *O* when the supporting springs are undeflected. The mass center *G* is defined by the coordinates $\left(x, y\right)$ with respect to the rotating frame. The position of the *i*th ball is given by the angle β_i relative to the mass center *G*. The reason for the choice of this rotating frame is that the equations of motion expressed in this frame are autonomous.

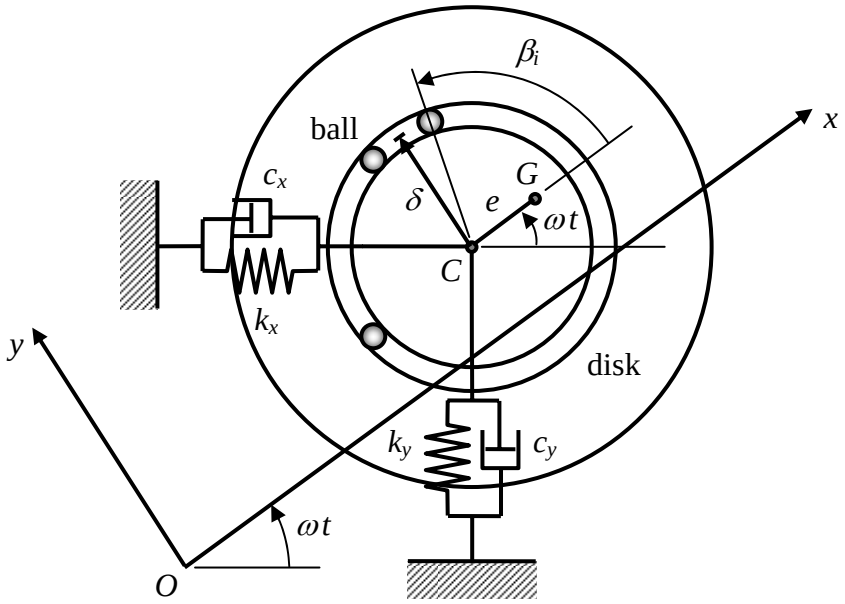

Figure 1 – Schematic of the system and co-rotating reference frame

The equations of motion are derived from Lagrange's equations given by

$$\frac{d}{dt}\left(\frac{\partial T}{\partial \dot{q}_k}\right)-\frac{\partial T}{\partial q_k}+\frac{\partial V}{\partial q_k}+\frac{\partial R}{\partial \dot{q}_k}=0\,, \tag{1}$$

where T is the kinetic energy, V the potential energy, R Rayleigh's dissipation function, and q_k the generalized coordinates. The kinetic energy can be expressed as

$$\begin{aligned} T=&\frac{1}{2}J\omega^2+\frac{1}{2}M(\dot{x}^2+\dot{y}^2+2\omega\, x\dot{y}-2\omega\,\dot{x}y+\omega^2x^2+\omega^2y^2)\\ &+\frac{1}{2}m_d(2\omega\, e\dot{y}+2\omega^2ex+\omega^2e^2)+\frac{1}{2}m_b\sum_{\mathrm{i}=1}^{3}[\delta^2(\dot{\beta}_i+\omega)^2\\ &-2\delta(\dot{\beta}_i+\omega)(\dot{x}-\omega y)\sin\beta_i+2\delta(\dot{\beta}_i+\omega)(\dot{y}+\omega x)\cos\beta_i] \end{aligned} \tag{2}$$

where J is the moment of inertia of the equivalent rotor and $M=m_s+m_d+3m_b$ indicates the total mass of the system. The potential energy is given by

$$V=\frac{1}{2}K\left(x^2+y^2\right) \tag{3}$$

Rayleigh's dissipation function can be represented by

$$R=\frac{1}{2}C(x^2+y^2-2\omega\dot{x}y+2\omega x\dot{y}+\omega^2x^2+\omega^2y^2)+\frac{1}{2}c_b\delta^2\sum_{i=1}^{3}\dot{\beta}_i^2 \tag{4}$$

Substitution of Eqs. (2), (3) and (4) into Eq. (1) yields the nonlinear equations of motion as follows:

$$\begin{aligned} &M\ddot{x}-2M\omega\dot{y}+C\dot{x}+(K-M\omega^2)x-C\omega y\\ &\qquad -m_b\delta\sum_{i=1}^{3}[\ddot{\beta}_i\sin\beta_i+(\dot{\beta}_i+\omega)^2\cos\beta_i]=m_de\omega^2 \end{aligned} \tag{5}$$

$$M\ddot{y} + 2M\omega\,\dot{x} + C\dot{y} + (K - M\omega^2)y + C\omega x + m_b\delta\sum_{i=1}^{3}[\ddot{\beta}_i\cos\beta_i - (\dot{\beta}_i + \omega)^2\sin\beta_i] = 0 \quad (6)$$

$$\begin{aligned} m_b\delta^2\ddot{\beta}_i + C_B\delta^2\dot{\beta}_i + m_b\delta(\ddot{y}\cos\beta_i + 2\omega\,\dot{y}\sin\beta_i - \omega^2 y\cos\beta_i) \\ -m_b\delta(\ddot{x}\sin\beta_i - 2\omega\,\dot{x}\cos\beta_i - \omega^2 x\sin\beta_i) = 0 \end{aligned} \quad (7)$$

In order to simplify the subsequent analysis, the following dimensionless variables are introduced,

$$x^* = x/e, \quad y^* = y/e, \quad \delta^* = \delta/e, \quad t^* = t\omega_n$$

where $\omega_n = \sqrt{K/M}$ indicates the natural frequency of the system. The equations of motion in terms of the dimensionless variables defined above can be written in matrix form as:

$$\mathbf{M}\mathbf{q}'' + (\mathbf{C} + \mathbf{G})\mathbf{q}' + \mathbf{g} + \mathbf{f} = 0, \quad (8)$$

where $\mathbf{q} = [x^*, y^*, \beta_1, \beta_2, \beta_3]^T$, $(\ )'$ indicates differentiation with respect to t^*, and

$$\mathbf{M} = \begin{bmatrix} 1 & 0 & -\mu\eta\sin\beta_1 & -\mu\eta\sin\beta_2 & -\mu\eta\sin\beta_3 \\ 0 & 1 & \mu\eta\cos\beta_1 & \mu\eta\cos\beta_2 & \mu\eta\cos\beta_3 \\ -\mu\eta\sin\beta_1 & \mu\eta\cos\beta_1 & \mu\eta\delta & 0 & 0 \\ -\mu\eta\sin\beta_2 & \mu\eta\cos\beta_2 & 0 & \mu\eta\delta & 0 \\ -\mu\eta\sin\beta_3 & \mu\eta\cos\beta_3 & 0 & 0 & \mu\eta\delta \end{bmatrix}$$

$$\mathbf{C} = \begin{bmatrix} 2\varsigma & 0 & 0 & 0 & 0 \\ 0 & 2\varsigma & 0 & 0 & 0 \\ 0 & 0 & 2\varsigma_B\mu\eta\delta & 0 & 0 \\ 0 & 0 & 0 & 2\varsigma_B\mu\eta\delta & 0 \\ 0 & 0 & 0 & 0 & 2\varsigma_B\mu\eta\delta \end{bmatrix},$$

$$\mathbf{G} = 2\Omega\begin{bmatrix} 0 & -1 & -\mu\eta\cos\beta_1 & -\mu\eta\cos\beta_2 & -\mu\eta\cos\beta_3 \\ 1 & 0 & -\mu\eta\sin\beta_1 & -\mu\eta\sin\beta_2 & -\mu\eta\sin\beta_3 \\ \mu\eta\cos\beta_1 & \mu\eta\sin\beta_1 & 0 & 0 & 0 \\ \mu\eta\cos\beta_2 & \mu\eta\sin\beta_2 & 0 & 0 & 0 \\ \mu\eta\cos\beta_3 & \mu\eta\sin\beta_3 & 0 & 0 & 0 \end{bmatrix}$$

$$\mathbf{f} = \begin{bmatrix} (1-\Omega^2)x - 2\varsigma\,\Omega y - \mu\eta\,\Omega^2\sum_{i=1}^{3}\cos\beta_i - \mu\Omega^2 \\ 2\varsigma\,\Omega x + (1-\Omega^2)y - \mu\eta\,\Omega^2\sum_{i=1}^{3}\sin\beta_i \\ \mu\eta\Omega^2\left(x\sin\beta_1 - y\cos\beta_1\right) \\ \mu\eta\Omega^2\left(x\sin\beta_2 - y\cos\beta_2\right) \\ \mu\eta\Omega^2\left(x\sin\beta_3 - y\cos\beta_3\right) \end{bmatrix}, \quad \mathbf{g} = \begin{bmatrix} -\mu\eta\sum_{i=1}^{3}\dot{\beta}_i^2\cos\beta_i \\ -\mu\eta\sum_{i=1}^{3}\dot{\beta}_i^2\sin\beta_i \\ 0 \\ 0 \\ 0 \end{bmatrix},$$

in which

$$\eta = \frac{m_b \delta}{m_d e} \ , \ \Omega = \frac{\omega}{\omega_n}, \ \varsigma = \frac{C}{2M\omega_n}, \ \mu = \frac{m_d}{M}, \varsigma_B = \frac{C_B}{2m_b\omega_n}.$$

EQUILIBRIUM POSITIONS

The first step in analyzing a nonlinear system is to identify the equilibrium positions. Setting $\mathbf{q}' = 0$ and $\mathbf{q}'' = 0$ in Eq. (8), the location of the equilibrium positions $\tilde{\mathbf{q}} = [\tilde{x}, \tilde{y}, \tilde{\beta}_1, \tilde{\beta}_2, \tilde{\beta}_3]^T$ is given by $\mathbf{f}(\tilde{\mathbf{q}}) = 0$. This set of equations can be expressed explicitly as

$$\left(1-\Omega^2\right)\tilde{x} - 2\zeta\Omega\tilde{y} - \mu\eta\Omega^2\left(\cos\tilde{\beta}_1 + \cos\tilde{\beta}_2 + \cos\tilde{\beta}_3\right) = \mu\Omega^2 \tag{9}$$

$$2\zeta\Omega\tilde{x} + \left(1-\Omega^2\right)\tilde{y} - \mu\eta\Omega^2\left(\sin\tilde{\beta}_1 + \sin\tilde{\beta}_2 + \sin\tilde{\beta}_3\right) = 0 \tag{10}$$

$$\tilde{x}\sin\tilde{\beta}_i - \tilde{y}\cos\tilde{\beta}_i = 0, \quad i = 1,3 \tag{11}$$

To solve Eqs. (9)-(11), we introduce the polar coordinates $\tilde{x} = \tilde{r}\cos\tilde{\theta}$, $\tilde{y} = \tilde{r}\sin\tilde{\theta}$, and rewrite Eqs. (11) as

$$\tilde{r}\sin\left(\tilde{\beta}_i - \tilde{\theta}\right) = 0.$$

The above equations require that $\sin\left(\tilde{\beta}_i - \tilde{\theta}\right) = 0$ or $\tilde{r} = 0$. The solution $\tilde{r} = 0$ indicates that there is no residual vibration. The associated equilibrium positions are called the perfect balancing positions. In this paper, we concentrate on the stability of the perfect balancing positions. Substituting $\tilde{x} = \tilde{y} = 0$ into eqs. (9) and (10) yields

$$\cos\tilde{\beta}_1 + \cos\tilde{\beta}_2 + \cos\tilde{\beta}_3 = -1/\eta \tag{12}$$

$$\sin\tilde{\beta}_1 + \sin\tilde{\beta}_2 + \sin\tilde{\beta}_3 = 0 \tag{13}$$

Equation (12) indicates that $\eta \geq 1/3$. In other words, perfect balancing is possible only when the total eccentricity of the 3 balls is no less than that of the disk.The positions of the three balls cannot be determined uniquely from these two equations. In other words, there are infinitely many equilibrium positions for $\tilde{r} = 0$. The steady-state equilibrium positions depend on the initial conditions. However, if the position of one of the balls is given, say $\tilde{\beta}_3$, the positions of the other two balls can be determined uniquely. Then we proceed to study the stability of the perfect balancing positions.

STABILITY ANALYSIS

The stability of an equilibrium configuration can be determined by the eigenvalues of the associated linearized system if all the eigenvalues have negative real parts or at least one of the eigenvalues has a positive real part. The linearization fails when the linearized system has some eigenvalues with zero real parts and no eigenvalues with positive real parts. Figure 2 is a typical result showing the variation of the eigenvalues

of a perfect balancing equilibrium configuration with the rotation speed. As can be seen from the figure, when the rotation speed is lower than about 1.51, one eigenvalue has a positive real part. Hence, the perfect balancing position is unstable for $\Omega < 1.51$. On the other hand, when the rotation speed is higher than 1.51, one eigenvalue is zero while the other eigenvalues have negative real parts. Since none of the eigenvalues in this speed range have positive real parts, the stability of the perfect balancing configuration cannot be determined from the linearizd system. In this case, the center manifold theorem is employed to study the stability of the equilibrium configuration.

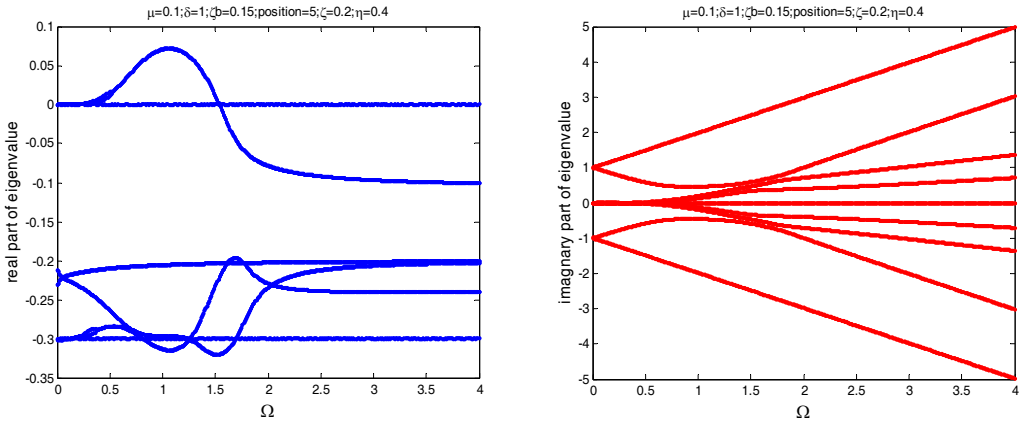

Figure 2 – Variation of eigenvalues with the rotation speed for a 3-ball balancer

In order to determine the center manifold, we first rewrite Eq. (8) into the standard form as

$$v_c = G\left(v_c, \mathbf{v}_s\right)$$
$$\mathbf{v}_s = \mathbf{J}_s \mathbf{v}_s + \mathbf{H}\left(v_c, \mathbf{v}_s\right)$$

where v_c is the coordinate associated with the eigenvalue 0, $\mathbf{v}_s$ a 9-dimensional vector, G a scalar function, $\mathbf{J}_s$ and $\mathbf{H}$ are 9×9 matrices. Further, $G\left(0,\mathbf{0}\right)=0$, $\mathbf{H}\left(0,\mathbf{0}\right)=0$, and the Jacobian matrices $DG\left(0,\mathbf{0}\right)=0$ and $D\mathbf{H}\left(0,\mathbf{0}\right)=\mathbf{0}$. There exists a local center manifold of the form $\mathbf{v}_s = \mathbf{h}\left(v_c\right)$, where $\mathbf{h}$ is a polynomial function of v_c [9]. By approximating the components of $\mathbf{h}$ with polynomials, the equation describing the dynamics of the one-dimensional center manifold can be expressed as $\dot{v}_c = \alpha_2 v_c^2 + \alpha_3 v_c^3 + O\left(v_c^4\right)$. The stability of the equilibrium configuration depends on the values of α_i. If $\alpha_2 \neq 0$, the equilibrium configuration is unstable. If $\alpha_2 = 0$ the equilibrium configuration is stable for $\alpha_3 < 0$ and unstable for $\alpha_3 > 0$.

RESULTS AND DISCUSSION

Previous investigations on the ball-type automatic balancer indicate that the rotation speed Ω, damping ratio ζ of the suspension, and damping ratio ζ_b of the ball-orbit

are important parameters influencing the performance of the automatic balancer. Therefore, we study the stability of the perfect balancing positions on the $\zeta - \Omega$ plane point by point. Stable areas in which perfect balancing positions are stable are identified.

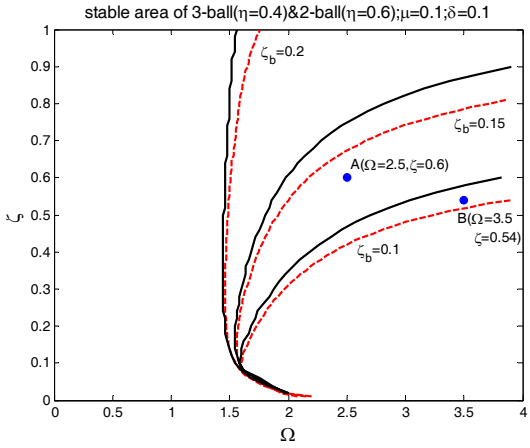

Figure 3 – Comparison of the stable areas of the 3-ball (*solid*) *and 2-ball* (*dashed*) *balancers*

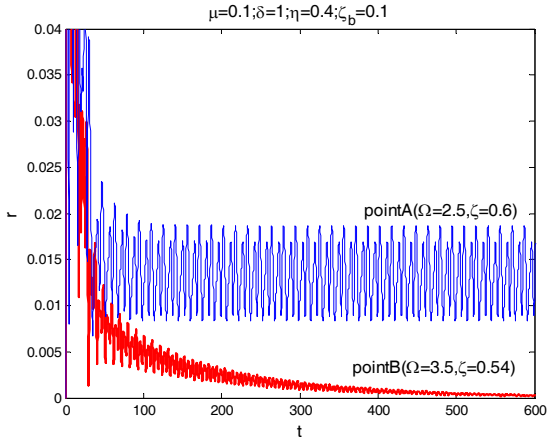

Figure 4 – Radial vibrations of the 3-ball balancer at points A and B

Figure 3 compares the stable areas of the 3-ball and 2-ball balancers for various values of ζ_b. The solid and dashed lines indicate the boundary of the stable area for the 3-ball and 2-ball balancers, respectively. For example, when $\zeta_b = 0.1$, the perfect balancing positions associated with point *A* are unstable for both the two- and three-ball balancer; the perfect balancing positions associated with point *B* is stable for the three-ball balancer but unstable for the two-ball balancer. Time responses of the nonlinear system with the three-ball balancer associated points *A* and *B* are computed numerically to verify the stable area obtained. The results for $\zeta_b = 0.1$ are shown in Fig. 4. It can be seen that the perfect balancing positions associated with point *A* are unstable while those with point *B* are stable. This verifies the results shown in Fig. 3. Further, as can be seen from Fig. 3, the 3-ball balancer has a larger stable area than the 2-ball balancer. This, in turn, implies that the 3-ball balancer has better performance than the 2-ball balancer.

COCLUSION

Ball-type automatic balancers are employed widely by optical disk drive industry to suppress the vibrations induced by the eccentricity of the optical disk. Proper conditions under which perfect balancing is possible are closely related to the stability of the perfect balancing positions of the automatic balancer. This paper investigates the stability of the perfect balancing positions of a three-ball automatic balancer. The stability is studied point by point on a parameter plane. The results indicate that the three-ball balancer has a larger stable area and hence better performance compared to the two-ball balancer.

ACKNOWLEDGEMENTS

This work was supported by the National Science Council of R.O.C. under grant NSC94-2212-E-002-033.

REFERENCES

[1] Bövik P. and Högfors C., "Autobalancing of Rotors," *Journal of Sound and Vibration*, **111**(3), pp. 429-440 (1986).

[2] Rajalingham C., Bhat R.B. and Rakheja S., "Automatic Balancing of Flexible Vertical Rotors Using a Guided Ball," *International Journal of Mechanical Science*, **40**(9), pp. 825-834 (1998).

[3] Lee J. and Moorhem W.K. V., "Analytical and Experimental Analysis of a Self-Compensating Dynamic Balancer in a Rotating Mechanism," *ASME Journal of Dynamic Systems, Measurement, and Control*, **118**, pp. 468-475 (1996).

[4] Chung J. and Ro. D.S., "Dynamic Analysis of An Automatic Dynamic Balancer for Rotating Mechanisms," *Journal of Sound and Vibration*, **1999**, pp. 1035-1056 (1999).

[5] Kang J-R, Chao C-P, Huang C-L, and Sung C-K, "The Dynamics of a Ball-Type Balancer System Equipped with a Pair of Free-Moving Balancing Masses," 2001, **123**, pp. 456-465 (2001).

[6] Huang W.-Y, Chao C.-P., Kang J.-R., and Sung C.-K., "The Application of Ball-Type Balancers for Radical Vibration Reduction of High-Speed Optical Disk Drives," *Journal of Sound and Vibration*, **250**(3), 415-430 (2002).

[7] Kim, W., Lee D.-J., and Chung J, "Three-dimensional Modeling and Dynamic Analysis of an Automatic Ball Balancer in an Optical Disk Drive," *Journal of Sound and Vibration*, **285**, 547-569 (2005).

[8] Chao C.-P., Sung C.-K., and Wang C.-C., "Dynamic Analysis of the Optical Disk Drives Equipped with an Automatic Ball Balancer with Consideration of Torsional Motions, " *ASME Journal of Applied Mechanics*, **72,** 826-842 (2005)

[9] Carr J., *Applications of Centre Manifold Theory*. (Springer-Verlag, New York, 1981).